Nitrous oxide and methane concentrations and air-sea fluxes in undersampled areas of the Mediterranean basin

Mercedes de la Paz[1], Susana Flecha[2], Fatima Zohra Bouthir[3], Milad Fahkri[4], Abed El Rahman Hassoun[4,5], Valeria Ibello[6], Korhan Özkan[6], Fiz F. Pérez[1], Adil Chair[3], Iris E. Hendriks[7]

1 Instituto de Investigaciones Marinas (IIM-CSIC), Vigo, Spain
2 Instituto de Ciencias Marinas de Andalucía (ICMAN-CSIC), Puerto Real, Cádiz, Spain
3 Institut National de Recherche Halieutique (INRH), Casablanca, Morocco
4 National Centre for Marine Sciences, National Council for Scientific Research in Lebanon (CNRS-L), Beirut, Lebanon
5 GEOMAR Helmholtz Centre for Ocean Research Kiel, Kiel, Germany
6 Middle East Technical University, Institute of Marine Sciences, Mersin, Türkiye
7 Climate Change Research Group. Mediterranean Institute for Advanced Studies (IMEDEA-CSIC), Esporles, Spain
Correspondence to: **Mercedes de la Paz Arándiga. E-mail:** mercedes.delapaz@iim.csic.es

Formatted: Spanish

Formatted: Spanish

Abstract: Nitrous oxide (N_2O) and methane (CH_4) are potent greenhouse gases for which oceanic contributions remain uncertain, particularly in undersampled regions like the Southwest and Southeast margins of the Mediterranean Sea, where there is a major observational gap. This data paper presents a comprehensive dataset of monthly N_2O and CH_4 concentrations and air-sea fluxes collected over a full seasonal cycle (April 2023 - June 2024 at most sites, with one station extended to September 2024) from eight coastal stations across three distinct Mediterranean ecoregions (Alboran, Balearic, and Levantine Seas) as part of the ROADSTER collaborative project. Sampling, preservation, and analytical procedures were standardized across sites, and dissolved-gas analyses were performed in a single laboratory to ensure comparability. We detail standardized sampling and analytical methodologies, including ancillary variables (temperature, salinity, dissolved oxygen, chlorophyll *a* and inorganic nutrients). The complied dataset reveals distinct seasonal and spatial variability: N_2O concentrations exhibit a strong negative correlation with temperature, with all stations acting as moderate N_2O sources. Conversely, CH_4 concentrations show greater variability and a positive correlation with temperature, with the Levantine sub-basin stations displaying episodic high-flux events (up to 35.20 μmol m^{-2} d^{-1}) indicative of localized seafloor sources. This dataset bridges significant data gaps in the Mediterranean, providing a crucial baseline for regional climate modeling, understanding biogeochemical processes, and future climate change impact assessments.

Keywords: Nitrous oxide, Methane, Greenhouse gases data, Mediterranean Sea, Coastal Ocean, Air-sea fluxes, Marine biogeochemistry

1. Introduction

Methane (CH_4) and nitrous oxide (N_2O) play critical roles in the atmospheric radiative balance and the climate system (Ciais et al., 2013). Although their atmospheric budgets are largely controlled by terrestrial sources and sinks, oceanic emissions represent an important component of their global cycling, particularly in coastal regions where emissions of N_2O and CH_4 are being enhanced (Weber et al., 2019; Saunois et al., 2020). The last synthesis of greenhouse gases (GHG) fluxes in the global coastal ocean developed by the Regional Carbon Cycle Assessment and Processes (RECCAP2), evidenced that emissions of CH_4 and N_2O from the global coastal ocean can offset a substantial fraction of the coastal uptake when expressed in CO_2 equivalent radiative forcing, highlighting the need to consider additionally N_2O and CH_4 gases when evaluating ocean–climate feedbacks (Rosentreter et al., 2021; Resplandy et al., 2024).

The ocean thus acts as both a source and a sink of CH_4 and N_2O through a range of interacting biogeochemical and microbial processes (Reeburgh, 2007; Codispoti, 2010). Global coastal and oceanic CH_4 emissions are estimated at approximately 12 (6–20) Tg CH_4 yr^{-1}, arising from microbially mediated production in marine sediments and the water column, as well as from geological pathways, including hydrothermal vents, cold seeps, mud volcanoes and CH_4 clathrate seepages (Reeburgh, 2007; Saunois et al., 2025). As a consequence, coastal ecosystems are increasingly recognised as weak but spatially extensive net sources of CH_4 to the atmosphere (Weber et al., 2019; Saunois et al., 2020). Similarly, the ocean accounts for about one-third of the natural N_2O sources to the atmosphere (Ciais et al., 2013). This gas is microbially produced in the ocean mainly through nitrification and denitrification, which are highly sensitive to dissolved oxygen levels, dissolved inorganic nitrogen (DIN) and redox conditions (Codispoti, 2010; Freing et al., 2012).

In this context, the Mediterranean Sea constitutes a particularly relevant system for investigating marine CH_4 and N_2O dynamics. As a semi-enclosed basin with an extensive coastline but narrow continental shelf, there are distinct biogeochemical and hydrodynamic characteristics and it is recognised as a climate-change hotspot (MedECC, 2020; Hassoun et al., 2025). Despite accounting for less than 1% of the global ocean surface, the Mediterranean hosts a disproportionately high biodiversity and is highly vulnerable to global warming, ocean deoxygenation, acidification, and increasing terrestrial nutrient and organic matter inputs, especially in coastal zones (Bianchi and Morri, 2000; Mouillot et al., 2011; Hassoun et al., 2025). These pressures are particularly pronounced in the western Mediterranean, subject to intense coastal development and tourism, that has seen a dramatic increase in pollution and habitat degradation, with only a small fraction of its coastline remaining in pristine condition (EEA, 2020). Furthermore, the warming rates are not uniform across sub-basins; sea surface temperature warms faster in the Eastern Mediterranean (~0.048 °C/year) than in the Western Mediterranean (~0.036 °C/year) (Pisano et al., 2020). Conversely, the upper water column (5–700 m) warms faster in the Western basin (~0.070 °C/year). Hence, all drivers of environmental change are expected to affect future biogeochemical cycles and emissions of N_2O and CH_4 in the Mediterranean Sea.

Despite its ecological importance and vulnerability, the Mediterranean Sea remains understudied regarding non-CO_2 GHG emissions. Data availability of N_2O and CH_4 and is extremely scarce compared to other oceanographic regions, as evidenced by the RECCAP2 synthesis report of GHG in global coastal oceans, with only a few measurements available for the emission computations of N_2O and CH_4 (Resplandy et al., 2024). Also, previous studies assessing the N_2O and CH_4 patterns throughout the water column are limited to the western limit of the Mediterranean Basin, namely at the Gibraltar Strait, where the impact of vertical mixing at surface N_2O concentrations drives short-term temporal variability (de la Paz et al., 2015), the Balearic Ocean Acidification Time Series (BOATS), where monthly observations show interannual and seasonal variability of N_2O and CH_4 since 2018 (Flecha et al., 2023; Flecha et al. 2025) and minor CH4 source from seagrass meadow reported in Corsica (Champenois et al., 2021). Although studies on GHGs' vertical patterns in water columns in the Eastern Mediterranean are very limited (Bange et al 1996), there is multiple evidence of gas released from geological sources of CH_4 at the Eastern Mediterranean Seafloor, where there are gas seepages and mud volcanoes, pointing out the high gas hydrate potential of the Eastern Mediterranean Sea (Merey and Longinos, 2019).

Expanding data collection in under-observed marine regions for non-CO_2 greenhouse gases, such as N_2O and CH_4, is valuable given their significant contributions to global warming and ocean feedback mechanisms (Bange et al., 2019; Hassoun et al., 2024). In the Mediterranean Sea, data scarcity—together with the limited temporal and vertical resolution of existing observations—still hampers basin-wide extrapolations and a comprehensive understanding of ocean–atmosphere fluxes of these gases (Rosentreter et al., 2023; Resplandy et al., 2024). These observational gaps are further compounded by the lack of long-term, sustained resources for key databases such as MEMENTO, constraining our ability to assess variability and detect trends in N_2O and CH_4 distributions and fluxes (Rees et al., 2022).

To bridge these limitations, strengthening coordination among scientists working across the Mediterranean basin is essential for improving data coverage and advancing measurements and predictions of non-CO_2 GHG dynamics (Bange et al., 2019; Hassoun et al., 2022). Standardising measurement protocols and ensuring the availability of long-term, high-quality datasets are fundamental steps for reducing analytical biases and for improving our understanding of N_2O and CH_4 processes (Wilson et al., 2018; Bange et al., 2019). Establishing a more integrated ocean-observing network in the Mediterranean region will enhance the consistency of data collection and contribute to the development of a Findable, Accessible, Interoperable and Reusable (FAIR;

Tanhua et al., 2019) data baseline. Such harmonised and traceable observations are prerequisite for robust assessments of oceanic greenhouse-gas fluxes, for reducing uncertainties in emission estimates, and for supporting transparent reporting under international and regional policy frameworks, including the Paris Agreement and its Global Stocktake (UNFCCC, 2015; UNFCCC, 2023).

As a product of the collaborative project between Eastern and Western Mediterranean countries entitled "Greenhouse Gas dynamics on the southern coasts of the Mediterranean Sea" (ROADSTER), this study provides a comprehensive dataset of monthly N_2O and CH_4 concentrations and fluxes across vast, understudied areas of the Mediterranean Sea—the southwest and southeast margins—over a full seasonal cycle. All gas measurements in seawater were performed in the same laboratory, and sampling and storage protocols were standardised across participants to minimise analytical bias (Wilson et al., 2018). This dataset offers the first combined assessment of seasonal and temporal variability of N_2O and CH_4 across three Mediterranean ecoregions, providing a robust baseline for understanding the processes driving temporal variability, informing future sampling strategies, and supporting global biogeochemical modelling and upscaling efforts aimed at refining estimates of oceanic CH_4 and N_2O emissions under ongoing climate and ocean-warming conditions.

2. Methods

The ROADSTER project, involving various research institutions from countries bordering the Mediterranean Sea (namely Lebanon, Morocco, Türkiye, and Spain), aimed to conduct a year-long series of monthly surface water measurements of N_2O and CH_4 at established coastal oceanographic stations. Sampling was conducted monthly at eight oceanographic stations across the Mediterranean, which were categorised into three marine regions: the Levantine Sea (Lebanon: LEV-B1, LEV-BEY2, and Türkiye: LEV-ETS), Balearic Sea (Spain: BAL-CA, BAL-CS, and BAL-PB), and Alboran Sea (Morocco: ALB-M'DIQ and ALB-REM).

Measurements encompassed dissolved N_2O and CH_4, along with ancillary variables pertinent to the biogeochemical cycles of N_2O and CH_4, such as temperature (T), salinity (S), dissolved oxygen (O_2), chlorophyll *a* (Chl*a*), and inorganic nutrients (nitrite, nitrate, phosphate and silicate). At the start of the project, detailed standardised protocols for the collection, preservation, and storage of gas samples until analysis were disseminated to participating laboratories. Additionally, the standardised equipment for gas sampling were distributed to ensure methodological consistency across participating laboratories and sampling initiatives.

2.1 Site description and sampling strategy

2.1.1 Morocco

The Mediterranean coast of Morocco was surveyed for 13 months from April 2023 to May 2024 at two sites, which are conditioned by the public health protection vocation of the INRH (National Institute for Fisheries Research) network, i.e. in the vicinity of shellfish production areas in the coastal domain. The stations, namely ALB-M'DIQ and ALB-REM, are located in the region of the Alboran Sea, characterised by the entrance of surface North Atlantic Water in the upper layer entering to the Mediterranean coinciding with the outflow of Mediterranean Water at the deeper layer, and the consistent presence of eddies and coastal upwelling that are modulated by mesoscale wind regime and complex hydrodynamics in the nearby Strait of Gibraltar (Macias et al, 2006).

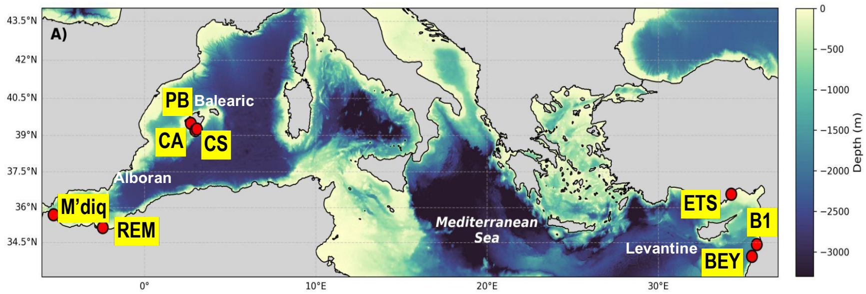

BAL-PB: Bay of Palma (Spain)
BAL-CA: Cabrera (Spain)
BAL-CS: Cape Ses Salines (Spain)
ALB-M'DIQ: M'diQ (Morocco)
ALB-REM: Ras El-Ma (Morocco)
LEV-ETS: Erdemli Time Series (Türkiye)
LEV-BEY: Beirut (Lebanon)
LEV-B1: Batroun (Lebanon)

Figure 1. Map of the Mediterranean Sea showing the locations of sampling sites (red dots) and the acronyms used in the text.

The ALB-M'DIQ station is characterized by a typically Mediterranean climate, influenced by offshore Mediterranean water masses and by episodic deep-water upwelling, with an annual mean temperature of 12.5°C and an annual total precipitation of 143 mm in 2023 (https://fr.tutiempo.net/climat/ws-603400.html). The site is located 800 m from the coast, with 10 m bottom depth, and was characterized by the highest content of sandy-silt, with no vegetation. The site is near the fishing harbor and marina in the town of M'diq, with a population of c. 100.000, and is subject to various anthropic pressures such as aquaculture activities and to effluent discharges, especially in summer.

The ALB-REM station is located in the north-east of Morocco, with a typically Mediterranean and dry climate, an annual mean temperature of 19.9°C and an annual total precipitation of 374 mm in 2023 (https://fr.tutiempo.net/climat/ws-603400.html). The site is located 1 km from the coast, over 30 m bottom depth and on a continental shelf with a gentle slope, consisting of sandy bottom without any vegetation, and 10 km west of the estuary of the Moulouya river (600 km long and the second largest in the North African coast only behind the Nile Delta). The site is near the fishing harbor of the Ras El-Ma village with a population of c. 20.000. Both sites are close to ports and fish farms.

Samples for N_2O and CH_4, Chl *a*, and inorganic nutrients were collected onboard an INRH small vessel. Water samples were collected using Niskin bottles at a depth of approximately 1 m. Hydrological parameters were measured using a Pro DSS Multiparametric sensor (Table 1).

2.1.2 Spain

Physicochemical and biogeochemical data were collected from three stations in the Balearic Sea, part of the Balearic Ocean Acidification Time Series (Flecha et al., 2022). The first station, located in the Bay of Palma (BAL-PB: ~30 m bottom depth), is part of the Balearic Islands Coastal Observing and Forecasting System monitoring network (SOCIB; https://www.socib.es/). Hourly measurements of temperature, salinity and O_2 were recorded with autonomous sensors. The second station is located in the Bay of Santa Maria, Cabrera Archipelago National Park (BAL-CA: ~8 m depth), a pristine area under governmental protection. Similar parameters (temperature, salinity, pH and O_2) were measured with high-precision sensors. Both BAL-PB and BAL-CA are fixed monitoring stations, with data collected monthly from depths of 1 and 4 m, respectively. The third site is in the coastal area near the Cape Ses Salines lighthouse (BAL-CS: ~2 m bottom depth), where surface water samples were collected biweekly, starting in August 2022 for O_2 measurements. Samples for dissolved CH_4 and N_2O concentrations and inorganic nutrients were also collected at all sites. Inorganic nutrient samples were analyzed using the Autoanalyser AA3 HR (Seal Analytical) via continuous-flow analysis. The precision, estimated from the coefficient of variation based on replicate analyses of the same water samples (n = 10), ranged from 0.13 % to 0.5 %.

The BOATS network surface layer is characterized by Modified Atlantic Water (MAW). There is no continuous freshwater contribution or significant anthropogenic pressures in BAL-CA or BAL-CS. Although BAL-PB could be affected by anthropogenic activities due to its proximity to urban areas, previous data analysis in this time series show no significant differences among stations for N_2O and CH_4 (Flecha et al., 2023; Flecha et al., 2025). Water samples were collected at BAL-PB and BAL-CA using a water pump and at BAL-CS directly from the coast (Table 1).

2.1.3 Lebanon

Samples in Lebanon were collected from two coastal stations: 1) LEV-B1 is located offshore Batroun city, Northern Lebanon (Table 1, Fig. 1) and is an inshore time-series station close to Batroun's port with a maximum depth of ~8 m, 2) LEV-BEY is a coastal station located offshore of Beirut, the Lebanese capital, and is surrounded by many infrastructure facilities (mainly recreational ones). Monthly monitoring of key physic-chemical parameters has been conducted since 1991 at station LEV-B1 (Hassoun et al., 2021) and for 30 years ago at station LEV-BEY. Both stations are sampled on a monthly basis and include measurements of a broad range of physical, chemical, and biological parameters. In addition, analysis of temperature records since 1999 indicates a significant warming trend of approximately 0.09 °C per year (Ouba et al., 2016).

The thermohaline properties were similar to those of the Levantine Sea Water source type. Sampling was conducted monthly between May 2023 and June 2024 to collect surface water samples. *In situ* temperature measurements were conducted using a standard surface thermometer. Salinity was determined using a Beckman salinometer, model R S7-C, with a precision of ± 0.01°C for temperature and ± 0.1 for salinity. For O_2 analysis, samples were first extracted from the Niskin bottle and concentrations were determined using Winkler titration (Hansen, 1999), with a precision of ± 15 μmol kg^{-1}. Phosphate concentrations were measured according to the method described by Murphy and Riley (1962) using a ThermoSpectronic Helios spectrophotometer, with a precision of ± 0.015 μmol kg^{-1}. Nitrites (N–NO_2) based on the method described by Bendshneider and Robinson (1952) and Nitrates (N–NO_3) following the method of Strickland and Parsons (1968), with a small modification from Grasshoff, (1961). Samples for total Chl *a* were filtered (Whatman GF/C) at a low pressure, and pigments were then extracted in 90% acetone and determined by a spectrophotometer according to Lorenzen (1967).

In LEV-B1 and LEV-BEY, observed biogeochemical variability is strongly influenced by seasonal and interannual changes in phytoplankton biomass, organic matter cycling, and episodic nutrient inputs. Previous studies in Lebanese coastal waters show recurrent spring and autumn chlorophyll-*a* maxima, reflecting enhanced primary production driven by winter mixing, transitional stratification, and episodic nutrient supply (Ouba et al., 2016). In addition, land-derived nutrient and organic matter inputs, including river discharge, coastal runoff, and wastewater effluents, have been identified as important local drivers modulating productivity and biogeochemical signals along the Lebanese margin (Abboud-Abi Saab et al., 2012; Hassoun et al., 2019).

2.1.4 Türkiye

Seawater samples were collected at the most Eastern Mediterranean coast of Türkiye (LEV-ETS), a highly oligotrophic area, dominated by the Asian Minor Current flowing from east to west in the offshore waters (Fach et al. 2021). The LEV-ETS station is situated 600 meters from the coastline, at a depth of 25 m, on a continental shelf characterized by a gentle slope and a sandy bottom devoid of vegetation. It is located near the town of Erdemli, which has a population of approximately 150,000. The area is subject to coastal eutrophication due to urban and agricultural pressures from the surrounding catchment area. The site is located 800 m east of Lamas River with an annual average discharge of 2.3 m^3 s^{-1} between 2010-2015 (General Directorate of State Water Affairs). The site has a hot, dry Mediterranean climate with an annual mean temperature of 19°C and an annual total precipitation of 569 mm (Turkish State Meteorological Service, 2024, https://mgm.gov.tr/, accessed August 1, 2024). The site has been monitored monthly between June 2023 to September 2024 by METU Institute of Marine Sciences. Based on a ten-year average of physic-chemical measurements (n = 2735), the site is characterized by a 22.65 ± 4.7 ℃ water temperature, 39.02 ± 0.63 salinity, ±225.6 ± 24.3 μmol kg^{-1} for O_2, 0.86 ± 0.96 μM for DIN and 0,38±0,35 μg L^{-1} for Chl *a*. The samplings cruises were conducted onboard RV-Lamas and water samples were collected using Niskin bottles at c. 1-2 m depth. CTD casts were made using Seabird or YSI Exo2 sensors. Due to logistical issues with the CTD, there are certain months (n=5) with missing salinity and temperature. The N_2O and CH_4 gas samples from these specific cruises were still taken into consideration in our study while temperature and salinity were filled with data from the Mediterranean Sea Physical Reanalysis Product (MEDSEA_MULTIYEAR_PHY_006_004; Escudier et al., 2020) and compared with the climatological time series of temperature and salinity, with good agreement.

Table 1. Country, station code and nearest city and code of the sampling sites, geographic coordinates, sampling period for N_2O and CH_4, number of cruises, ancillary variables.

Country Oceanographic region	Site Station Code	Location	Bottom Depth (m)	Gases Sampling period	Sampling cruises (n)	Ancillary Variables	Research Institution cruises
Spain Balearic Sea	Cabrera BAL-CA	39.15 ºN 2.95 ºE	8	05/2023 06/2024	13	T, S, Nuts, O_2, Chl *a*	IMEDEA-CSIC
	Cape Salines BAL-CS	39.27 ºN 3.05 ºE	2	05/2023 06/2024	13	T, S, Nuts, O_2, Chl *a*	IMEDEA-CSIC
	Palma Bay BAL-PB	39.49 ºN 2.70 ºE	30	05/2023 06/2024	13	T, S, Nuts, O_2, Chl *a*	IMEDEA-CSIC
Lebanon Levantine Sea	Batroun LEV-B1	34.42 ºN 35.75 ºE	8	05/2023 06/2024	12	T, S, Nuts, O_2, Chl *a*	CNRS-L
	Beirut LEV-BEY	33.90 ºN 35.47 ºE	3	05/2023 06/2024	14	T, S, Nuts, Chl *a*	CNRS-L
Türkiye Levantine Sea	Erdemli Time Series LEV-ETS	36.56 ºN 34.25 ºE	25	06/2023 09/2024	12	T, S	METU-IMS
Morocco Alboran Sea	M'diq ALB- M'diq	35.69 ºN -5.32 ºE	10	04/2023 04/2024	13	T, S, Nuts, O_2, Chl *a*	INRH
	Ras El Ma ALB-REM	35.15 ºN -2.45 ºE	30	04/2023 04/2024	13	T, S, Nuts, O_2, Chl *a*	INRH

2.2 Dissolved N_2O and CH_4 measurements

To ensure consistency across all sites, identical sampling materials and detailed protocols for N_2O and CH_4 were prepared and distributed to each collaborating laboratory. Before the start of the sampling cruises, dedicated training sessions on trace gas sampling were provided to all teams, aiming to harmonize procedures and minimize potential biases between sites and laboratories. Duplicate samples for N_2O and CH_4 were collected in 120 mL borosilicate serum vials, sealed with grey chlorobutyl septa and aluminium crimps. To preserve the samples, approximately 200 µL of saturated $HgCl_2$ solution was added and the vials were stored upside down in the dark until analysis at the AQUANITROMET laboratory (de la Paz and Pérez, 2026) of the Instituto de Investigaciones Marinas (IIM-CSIC, Vigo, Spain).

The dissolved concentrations of N_2O and CH_4 were analysed using the static-headspace equilibration technique combined with gas chromatography following de la Paz et al., (2015, 2021). It consists of creating a headspace by automatically introducing a volume (20 mL) of ultrapure N_2 gas into the sample vial using a high-precision automatic burette displacing the same volume out of the vial by piercing the septum with two needles. After reaching equilibrium overnight in a temperature-controlled environment, 18 mL of the headspace is automatically extracted using a high-precision burette and injected into a gas chromatograph (Agilent GC 7890-A), where the signal for each gas is separated using two independent Porapak Q-packed columns. Finally, N_2O is detected with an electron capture detector and CH_4 with a flame ionization detector. For the calibration curve, we used triplicate injections of three combined gas standard mixtures of N_2O and CH_4 in N_2, supplied by NOAA (National Oceanic and Atmospheric Administration) (N_2O:CH_4=332:1959 ppb) and by AirLiquide France (ratios N_2O: CH_4=1000:3000 and 3100:5000 ppb). The precision estimated from the averaged coefficient of variation of duplicates (n=123) for this study was 1% for N_2O and 4.5% for CH_4. Instrumental limits of detection (LOD) and quantification (LOQ) for GC were defined as 3 and 10 times the standard deviation of triplicate injections of the lowest standard (NOAA atmospheric level), divided by the calibration slope, respectively. This yielded LOD ranges of 3–10 ppbv for CH4 and 0.1–2.9 ppbv for N2O, and LOQ ranges of 9.8–32.4 ppbv for CH4 and 0.3–9.7 ppbv for N2O. Because dissolved gas analysis is fundamentally constrained by detector sensitivity, conservative methodological limits were calculated by substituting the maximum gas-phase LOD and LOQ values into Eq. 1 for seawater at S = 35 and T = 20 °C. The resulting aqueous LODs were 0.11 nmol L^{-1} (CH4) and 0.16 nmol L^{-1} (N2O), with corresponding LOQs of 0.35 nmol L^{-1} (CH4) and 0.55 nmol L^{-1} (N2O). This analytical system was intercalibrated with other laboratories, with very good results, as part of activities during the first large international experiment to compare marine N_2O and CH_4 measurements, organized by the Scientific Committee on Oceanographic Research (Wilson et al., 2018).

The gas concentration using the headspace equilibration was computed following Wilson et al. (2018):

$$C_{meas}\,[\mathrm{nmol\ L^{-1}}] = \left(\beta\, x\, PV_{wp} + \frac{xP}{RT}V_{hs}\right)/V_{wp} \qquad \text{Eq. 1}$$

where β denotes the Bunsen solubility coefficient of N_2O (Weiss and Price, 1980) and CH_4 (Wiesenburg and Guinasso, 1979) expressed in nmol L^{-1} atm^{-1}; x is the dry gas mole fraction (ppb) determined in the headspace; P is the ambient atmospheric pressure (atm); V_{wp} and V_{hs} are the volumes of the water sample and equilibrated headspace, respectively (mL); R is the universal gas constant (0.08205746 L atm K^{-1} mol^{-1}); and T is the equilibration temperature (K). The CH_4 and N_2O concentrations are also expressed as percent saturation (N_2OSat and CH_4Sat in %), calculated as the ratio between the measured concentration (C_{meas}) and the equilibrium concentration in seawater (C_{equi}) for each gas. The equilibrium concentrations were computed by multiplying Bunsen solubility coefficient (β) of each gas by the monthly average atmospheric molar fraction of N_2O and CH_4 measured at the Lampedusa monitoring station—the only site in the Mediterranean Sea with continuous records of these gases—obtained from the NOAA monitoring network (Lan et al., 2025).

Due to the lack of standardised QC tools or reference materials in aqueous phase for N_2O and CH_4, such as those available for the carbonate system (CRMs produced by A. Dickson at Scripps USA), our QC procedure relied on duplicates seawater samples and reported results as the coefficient of variation (CV, %). The presence of outliers was established based on the CV value between duplicates; hence, samples were discarded with a CV higher than 4.5% (n=3) for CH_4 and1% for N_2O (n=1). In addition, some glass flasks were broken during transport to Vigo (n=14), reducing the total number of duplicates samples.

2.3 Calculation of N_2O and CH_4 air-sea fluxes

The air-sea fluxes (F) were calculated using the following equation:

$$F = k_w\,(C_{meas} - C_{equi}) \qquad \text{Eq. 2}$$

where k is the gas transfer velocity (cm h^{-1}) and (C_{meas} – C_{equi}) is the air-sea concentration gradient of N_2O and CH_4, being C_{meas} and C_{equil} the measured and equilibrium gas concentrations defined in the previous section. By convention, and following the sign of the gas concentration gradient, negative values of F correspond to a transfer of N_2O or CH_4 from the atmosphere to the ocean (i.e., a sink for the atmosphere) and positive values of F correspond to a transfer of those gases from the ocean to the atmosphere (i.e., a source for the atmosphere). There is a long-term debate over which is the best expression for gas transfer rate k, but here we adopted as the expression given by Wanninkhof et al. (2014), since it is widely used in the last RECCAP2 analysis for GHG emissions in the coastal ocean (Resplandy et al., 2024). The gas transfer velocity by Wanninkhof (2014), gave the expression $k_w = 0.251<U^2> (Sc/660)^{-0.5}$, where $<U^2>$ is the average of the square wind speed and Sc is the Schmidt number (dimensionless). For our study, due to lack of local sources for wind data on land or buoy for some of the stations, we used the monthly averaged of the square of 6 hourly wind data provided by the Cross-Calibrated Multi-Platform Ocean Surface Wind Vector 3.0 (CCMP) wind data product that combines satellite and buoy data with model predictions (Mears et al., 2022). This wind speed product is the optimum choice using the k proposed by Wanninkhof (2014), which is computed using this same data product, and has been demonstrated to be an optimum wind source for coastal regions (Otero et al.,2013). The Sc, dependent on the temperature, salinity, and specific gas molecule, is calculated according to the coefficients for N_2O and CH_4 and the equation reported by Wanninkhof (2014). Then, the Schmidt number for the *in situ* salinity at the Mediterranean station was calculated by interpolating Sc for fresh water and seawater.

To determine the annual average air-sea fluxes of N_2O and CH_4 at each station, calculations were performed over a 12-month period. Missing monthly values of N_2O, CH_4, temperature, and salinity during this timeframe were reconstructed through temporal linear interpolation based on the closest available cruise measurements.

2.4 Analysis of the variability of spatial and temporal variability of N_2O and CH_4

To determine whether the differences in N_2O and CH_4 concentrations and other variables across stations were statistically significant, we used Tukey's test with a significance level of $p < 0.05$. Additionally, we compute the Spearman correlation coefficients between surface water CH_4 and N_2O concentrations and potential environmental factors, such as water temperature, salinity, dissolved oxygen, inorganic nutrients, and Chl *a.* All analyses were done using the R software.

3. Results

Besides specific N_2O and CH_4 measurements, we detail the environmental setting and primary oceanographic processes influencing the variability of measurements conducted in our study, while also providing initial insights for future in-depth biogeochemical studies in the region.

A total of 111 observations of N_2O and CH_4 were obtained between April 2023 and June 2024 (except for LEV-ETS, where observations were extended to September 2024), accompanied by measurements of temperature, salinity, dissolved oxygen, Chl *a*, and nutrients (NO_3, NO_2, PO_4, and SiO_2). Temporal coverage is uniform across stations, with one sampling event per month, except for minor gaps due to logistical problems with ship availability or inclement weather.

3.1. Seasonal variability of N_2O and CH_4 concentrations

Overall, the seasonal variability of sea surface temperature (SST) was very similar in every region, ranging from 14.5 °C in BAL-PB (March 2024) to 31.2 °C in LEV-BEY (August 2023) (Fig. 2). ALB-M'DIQ exhibits unique characteristics, particularly the unexpectedly low temperatures observed during the summer. These anomalies are likely linked to the eddy-driven vertical motion in the Alboran sub-basin. This connection is supported by several studies that have documented mesoscale eddies with intensified vertical motion and subsurface anticyclonic eddies along the African coast (Tintoré et al., 1991; Viudez et al., 1998). Hence, except for ALB-M'diq, the maximum (August) and minimum surface temperatures (from December to March) showed an overall synchronised cycle between the stations, with lower seasonal SST amplitudes in the southern coast of the Alboran sub-basin (9.5 °C ALB-REM) to higher seasonal SST amplitudes in the stations of the Balearic Sea (13.3 °C in BAL-PB).

The sea surface salinity ranged from 36.6 in BAL-CS in June 2024 to 39.5 in LEV-ETS (Fig. 2b). Compared to the other regions, the seasonal cycle of salinity was clearly observed in the surface waters of Lebanon, where both stations LEV-B1 and LEV-BEY showed higher salinity values from July to November, owing to intense evaporation and lower values from January to April owing to precipitation/continental runoff (Abboud-Abi Saab et al., 2012).

Seasonal variability in N_2O concentrations was observed at all stations, with concentrations increasing during winter and reaching minimum values in summer (Fig. 2, Table 2). The highest N_2O concentration of 9.95 nmol kg^{-1} was measured in BAL-PB in January 2024, whereas the minimum N_2O concentration of 6.3 nmol kg^{-1} corresponded to LEB-B1 in August of 2023. Monthly N_2O concentrations showed a clear intra-annual cycle, with amplitudes ranging from 1.3 nmol kg^{-1} in ALB-M'DIQ to 3.1 nmol kg^{-1} in BAL-PB Bay, which were directly correlated with SST amplitude. Despite some inter-station differences, the timing of the peaks and troughs was broadly consistent across the Mediterranean coast.

The CH_4 concentrations in surface waters ranged from 2.9 nmol kg^{-1} measured in March 2024 in BAL-CA to 38.2 nmol kg^{-1} measured in September 2023 in LEV-ETS (Table 2). The distribution of CH_4 concentrations were very skewed, and the minimum CH_4 was comparable between the stations (60% of values were lower than 5 nmol kg^{-1}), and CH_4 peaks were evenly distributed and consistently high along the coast of the Levantine sub-basin. Only BAL-CS showed a moderate seasonal trend, with a gradual increase in CH_4 concentrations in June, peaking in July, and gradually decreasing through September 2023. Apart from this, no clear seasonal pattern was observed for CH_4 concentrations.

The saturation status of N_2O in surface water for most of the period was oversaturated (Fig. 2, Table 2), except in May 2023 at the stations of the Balearic sub-basin (BAL-CS, BAL-CA) and in ALB-M'DIQ in October 2023 and May 2024 with a moderate seasonal trend of lower N_2OSat in winter and spring, and higher oversaturation in summer months, with the N_2OSat ranging from 96 ± 0% in BAL-CS in May 2023 and 127 ± 1% in LEV-ETS in September 2023. The surface water at all the stations was supersaturated in CH_4 (Fig. 2, Table 2), with minimum values during the winter and early spring (110±4% in BAL-CA in March 2024) and higher values in summer (up to 400%), with very high CH_4Sat peaks in the eastern Basin of the Levantine sub-basin that reached the 1973 ±4%

Table 2. Summary of the results using the entire database. The table shows the average, minimum (min), median, and maximum (max) values for temperature (°C), salinity, dissolved CH_4 concentration (nmol kg^{-1}), CH_4 saturation percent (CH_4 Sat %) dissolved N_2O concentration (nmol kg^{-1}), N_2O saturation percent (N_2O Sat %) in the surface water for every station

			Salinity	Temperature °(C)	CH_4 (nmol kg^{-1})	CH_4Sat (%)	N_2O (nmol kg^{-1})	N_2OSat (%)	Dissolved Oxygen (µmol kg^{-1})	Chl *a* (mg L^{-1})	Nitrate (µM)	Nitrite (µM)	Phosphate (µM)	Silicate (µM)
Balearic Sea	BAL-CA	Mean	37.40	20.4	3.8	168	8.1	105	228	0.06	0.18 ±	0.03	0.32	0.6
		±SD	±0.24	±4.7	±0.8	±48	±1.0	±4	± 20	± 0.07	0.12	± 0.04	± 0.53	± 0.2
		min	37.10	14.8	2.9	110	6.7	98	195.21	0.00	0.06	0.00	0.00	0.05
		max	38.00	27.5	5.6	277	9.3	110	254.93	0.16	0.38	0.14	1.91	0.69
	BAL-CS	Mean	37.42	21.5	4.7	211	7.8	104	235	0.08 ±	1.97 ±	0.05 ±	0.12 ±	0.5
		±SD	±0.42	±4.4	1.4±	±80	±0.9	±3	± 18	0.06	1.62	0.06	0.16	± 0.2
		min	36.60	15.1	2.9	113	6.6	9	209.39	0.00	0.23	0.00	0.01	0.07
		max	37.90	28.1	8.0	399	9.2	110	259.54	0.17	6.27	0.22	0.70	0.77
	BAL-PB	Mean	37.44	21.1	4.1	180	8.3	108		0.08 ±	0.36 ±	0.06 ±	0.18 ±	
		±SD	±0.21	±5.0	±0.8	±44	±1.1	±4	232 ± 17	0.09	0.47	0.05	0.23	1.1 ± 1.6
		min	37.10	14.5	3.0	129	6.8	101	208.88	0.00	0.03	0.01	0.00	0.41
		max	37.80	27.8	5.5	275	10.0	117	254.82	0.30	1.26	0.14	0.80	6.14
Levantine Sea	LEV-B1	Mean	38.80	24.5	6.9	323	7.3	111	212	0.19		0.06	0.99	2.1
		±SD	±0.39	±3.8	±1.7	±80	±0.6	±5	± 16	± 0.12	0.6 ± 0.62	± 0.04	± 2	± 1.2
		min	38.02	18.9	4.7	223	6.3	102	183.49	0.05	0.14	0.02	0.01	0.80
		max	39.24	30.4	10.5	516	8.2	118	241.98	0.53	2.64	0.15	6.23	5.61
	LEV-BEY	Mean	38.82	25.3	8.1	383	7.4	116	- -	0.45	1.21	0.1	0.07	2.2
		±SD	±0.36	±3.7	±5.2	±243	±0.5	±11		± 0.22	± 2.03	± 0.07	± 0.04	± 1.6
		min	38.32	20.1	4.4	192	6.4	106	- -	0.14	0.12	0.02	0.01	0.91
		max	39.26	31.2	18.2	900	8.0	145	- -	0.84	7.78	0.25	0.15	6.93
	LEV--ETS	Mean	39.23	24.2	13.6	659	7.2	112	- -	- -	- -	- -	- -	- -
		±SD	±0.46	4.6±	±9.8	±499	±0.7	±7						
		min	38.63	18.8	4.7	237	6.3	104	- -	- -	- -	- -	- -	- -
		max	39.56	29.8	38.2	1973	8.2	127	- -	- -	- -	- -	- -	- -
Alboran Sea	ALB-M'DIQ	Mean	37.18	17.7	4.9	199	8.5	104	245	0.27	0.44	0.09	0.07	0.3
		±SD	±0.33	±1.8	±1.5	±58	±0.3	±4	± 9	± 0.23	± 0.25	± 0.1	± 0.05	± 0.2
		min	36.75	15.6	3.6	142	7.7	97	231.45	0.00	0.05	0.01	0.03	0.03
		max	37.81	22.2	9.3	368	9.1	111	255.10	0.89	0.78	0.38	0.21	0.68
	ALB-REM	Mean	37.18	20.3	4.5	194	8.1	107	225	0.08	0.61	0.25	0.1	0.4
			±0.12	±3.2	±0.8	±37	±0.5	±4	± 12	± 0.07	± 0.43	± 0.28	± 0.06	± 0.2
		min	37.01	16.8	3.9	157	6.9	102	202.49	0.02	0.09	-0.08	0.05	0.09
		max	37.40	26.3	6.1	259	8.6	114	243.68	0.29	1.35	0.68	0.22	0.74

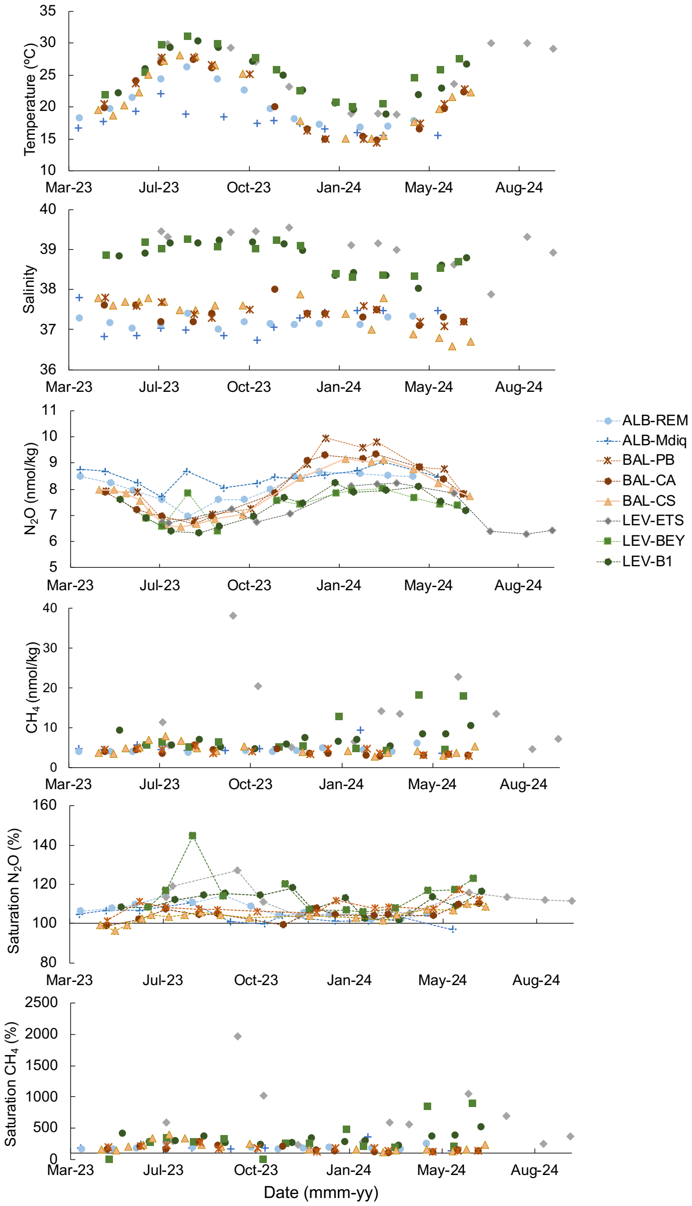

Figure 2. Time series data from the study sites, from top to bottom for temperature, salinity, dissolved N_2O and CH_4 concentration and saturation percent (expressed as nmol kg^{-1} and % saturation) over the sample period.

3.2. Spatial variability and annual mean regional distribution of N_2O and CH_4 on coastal waters on the Mediterranean Basin scale.

Sea Surface Temperature distribution was relatively homogeneous within each subbasin (Fig. 3) (Tukey test; $p > 0.05$). However, a significant longitudinal gradient was observed across the Mediterranean Sea. The mean SST increased from 17.7 ± 1.8 °C at the westernmost station (ALB-M'diq, Alboran Sea) to 25.6 ± 4.6 °C at the easternmost station (LEV-ETS, Levantine Sea). Consequently, SST values were significantly higher in the Levantine Sea (B1, BEY, and ETS) compared to those in the Alboran and Balearic sub-basins (M'Diq, REM, and CA; p < 0.05), while no significant differences were found between the latter two subbasins. A similar zonal trend was found for salinity, with mean values increasing from 37.18 ± 0.12 in Alboran coastal waters to 39.11 ± 0.46 in the Levantine sub-basin. This reflects a significant salinification in the Eastern basin (ETS, B1, and BEY) compared to the western Moroccan coast (M'diq, REM) and the Balearic sub-basin (CS, CA, PB), with a maximum inter-basin gradient of 1.9.

The regional distribution of CH_4 across the Mediterranean Sea exhibited a marked longitudinal contrast (Fig. 3). Although temporal variability was systematically higher in the eastern stations, significantly elevated mean CH_4 concentrations were only observed at LEV-ETS (13.6±9.8 nmol kg^{-1}; Tukey's test, $p < 0.05$). In the remaining stations, average concentrations ranged from 3.8±0.8 nmol kg^{-1} at BAL-CA to 8.1±5.2 nmol kg^{-1} at LEV-BEY. Despite the occurrence of high episodic values at LEV-B1 and LEV-BEY, their median concentrations did not differ significantly from those in the Alboran and Balearic sub-basins (Tukey's test, $p > 0.05$). Surface waters throughout the Mediterranean Sea were persistently supersaturated in CH_4, with mean saturation levels ranging from 168±46% (BAL-CA) to 659±500% (LEV-ETS), following the spatial pattern of absolute concentrations. The CH_4Sat oversaturation peaks along with their associated variability observed at the LEV-ETS station (up to 659±500%) suggest the influence of localised seafloor sources, such as cold seeps or shallow gas venting, which are well documented in the Levantine sub-basin (Colleman and Ballard, 2001). Alternatively, nearshore/river filaments or submarine groundwater discharge (SGD), which can be brackish to saline and may not show as a salinity minimum, can significantly raise CH_4, SST, and salinity remain mostly unchanged. In this region, the presence of coastal groundwater systems and SGD is supported by hydrogeochemical/isotopic evidence for the Mersin–Erdemli and Lamas areas (Kuyumcu, 2023). Both scenarios, seafloor sources and SGD, can likely contribute to the episodic enrichment of surface waters in this region, however further research is needed to confirm them.

In contrast, N_2O concentrations showed much lower spatial variability, with station averages ranging from 7.2±0.7 nmol kg^{-1} (LEV-ETS) to 8.5±0.3 nmol kg^{-1} (ALB-M'DIQ) (Table 2, Fig. 3). The N_2O distribution showed an inverse relationship with SST, and significant differences (Tukey, $p < 0.05$)

were observed only between the Eastern and Western extremes of the Mediterranean Sea. Notably, N_2OSat levels followed an opposite longitudinal trend to absolute concentrations, with higher values at the Eastern Basin (ranging from 100±4% at BAL-CS to 116±11% in the Levantine stations). Despite the widespread N_2O oversaturation, these values remain relatively low compared to those in other coastal seas (Charpentier et al., 2007; Sommer et al., 2025). This finding suggests that both external inputs and in situ biological production, such as nitrification and denitrification processes in the water column or benthic compartment, are comparatively weak in coastal waters of the studied stations, consistent with the ultra-oligotrophic nature of the Mediterranean Sea.

Nutrient concentrations reflected a predominantly oligotrophic regime, although episodic enrichment was observed near the coast (Table 2). Maximum values of nitrate (up to 7.78 μM 1 at LEV-BEY) and phosphate (up to 6.23 μM at LEV-B1) suggest localized continental influence. Specifically, the elevated silicate levels in the Eastern Basin (mean >2 μM) coupled with high nutrient peaks point towards terrestrial runoff and potential anthropogenic inputs from major coastal urban centers as the primary drivers of coastal nutrient variability. Nutrient stoichiometry indicated a shift from the typical phosphorus-limited regime of the open Mediterranean towards nitrogen-limited conditions in several coastal sites. Specifically, low N:P ratios (<10) in stations such as LEV-B1 and BAL-CA, coupled with high silicate concentrations (up to 5.61 μmol·L−1), suggest a strong influence of terrestrial runoff and urban effluents. This is consistent with the description of the study sites (Section 2.1), where the proximity of anthropogenic activities is identified as a potential driver of local biogeochemical variability. The highest phytoplankton biomass was recorded at LEV-BEY (mean 0.45±0.22 $\mu g \cdot L^{-1}$), where a more balanced N:P ratio (≈18.7) appears to support enhanced primary production compared to the more nitrogen-limited eastern sites.

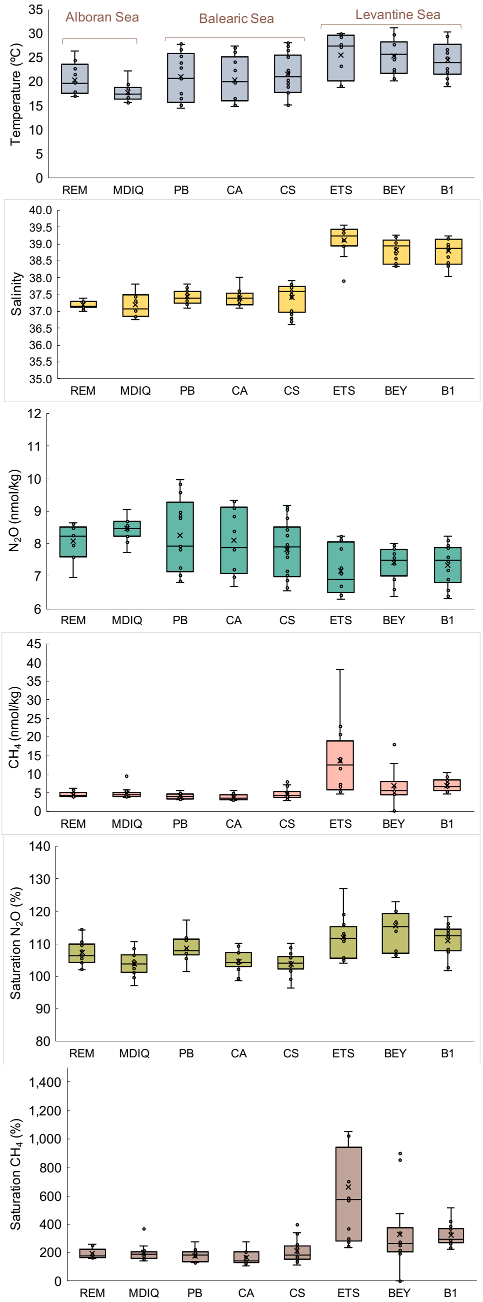

Figure 3. West to East spatial distribution surface temperature (ºC), salinity, concentration of N_2O and CH_4 in nmol kg^{-1} and saturation percentage of N_2O (N_2OSat) and CH_4 (CH_4Sat) across sampling stations (x-axis).

In each box-plot, the horizontal line represents the median, the cross indicates the mean, the box spans the interquartile range, and the whiskers extend to the data extremes. The listed acronyms correspond to: Ras El Ma= REM; M'diq=MDIQ, Palma Bay =PB; Cabrera =CA; Cape Salines= CS; Erdemli Time Series =ETS; Beirut=BE; Batroun =B1

3.3. Correlation of surface N_2O and CH_4 with environmental variables

The N_2O concentrations showed a strong negative correlation with temperature for the entire database collected from all study sites; showing that both the temporal and spatial scales of variability were highly controlled by temperature (Fig. 4). This negative correlation points to a thermodynamic control of the variability through solubility, which increases N_2O in colder water. However, there was a positive correlation between N_2OSat and temperature ($N_2OSat = 0.82*T+89.96$; $r=0.58$, $n=109$, $p<<0.01$), with higher values in summer in the Eastern Basin than in winter in the Western Basin, corresponding to an enhancement of N_2O microbial production with increasing temperature. In contrast, CH_4 concentrations showed the opposite behaviour to N_2O, with greater variability and a positive correlation with temperature, indicating mechanisms other than solubility controlling the variability and important sources of CH_4 in the Eastern Basin.

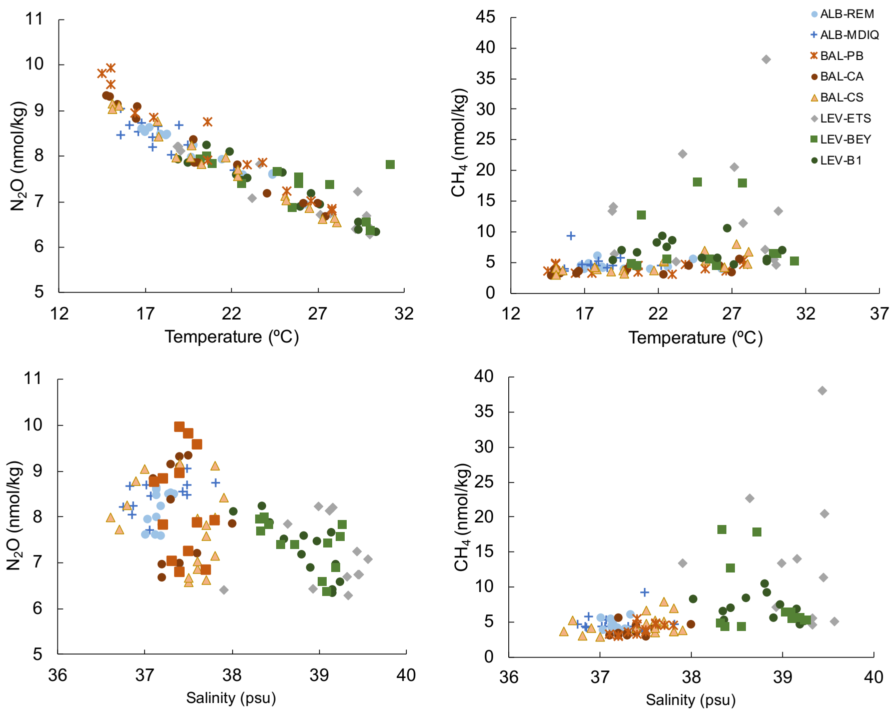

Figure 4. Scatter plots illustrating the relationship between dissolved N_2O and CH_4 concentrations (nmol kg^{-1}) and key environmental variables: surface water temperature (°C) and salinity. Data from all stations are included, highlighting the overall trends across the Mediterranean Basin

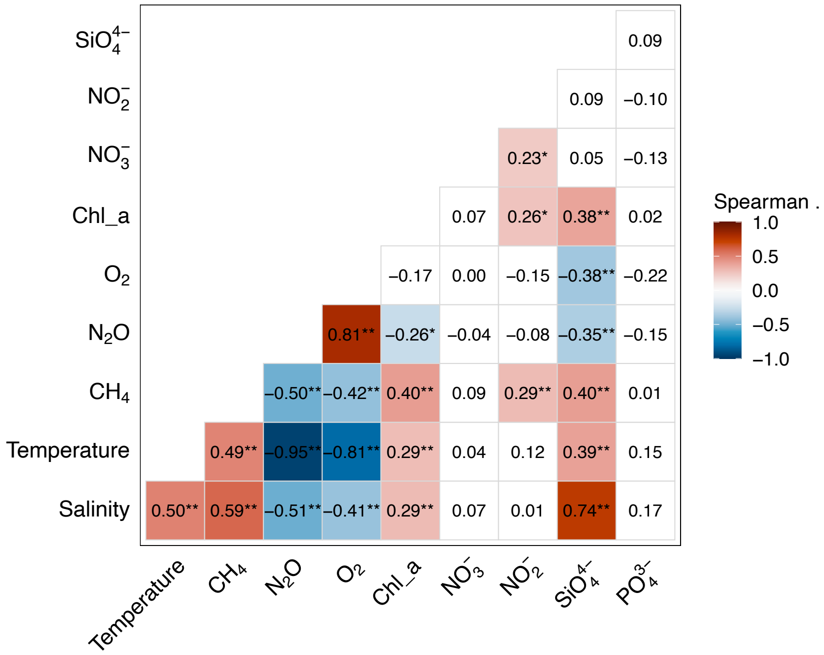

Figure 5. Spearman's rank correlation matrix showing the interrelationships between N_2O and CH_4 concentrations and various environmental parameters (temperature, salinity, dissolved oxygen, nutrients, chlorophyll *a*) for the entire dataset, excluding data from LEV-ETS due to missing ancillary variables. Significant correlations are indicated with asterisk (**:$p < 0.01$; *:$p < 0.05$).

The Spearman correlation matrix accounts for overall variability at both temporal and spatial scales, as shown in Fig. 5 for N_2O and CH_4 concentrations. The correlation analysis showed that N_2O was strongly correlated with temperature (-0.95, $p < 0.01$) and significantly negatively correlated with salinity (-0.51, $p < 0.01$), Chl *a* (-0.26, $p < 0.05$), and silicate (- 0.35). ($p < 0.01$) and was highly positively correlated with O_2 (r = 0.81, $p < 0.01$). The CH_4 showed an opposite behaviour, with a significant negative correlation with oxygen (-0.42, p<0.01) and positively correlation with salinity (r = 0.59, p<0.01), temperature (0.49, p<0.01), Chl *a* (0.4, p<0.01), and silicate (0.4, p<0.01). Temperature was clearly the main controlling factor, especially for N_2O, and the overall correlation with salinity was stronger than when the analysis was performed at every station. This could be due to the higher salinity in the Levantine Sea and the zonal distribution pattern of salinity in the basin itself. Furthermore, the analysis of the Spearman correlation matrix for each station revealed additional local mechanisms acting on the seasonal scale that could be relevant, such as a significant positive correlation in O_2 among Western Mediterranean stations (BAL-CA, BAL-CS, BAL-PB, and BAL-REM) that was not significant in the eastern Levantine sub-basin. In addition, the strong negative correlation between N_2O and temperature was ubiquitous across stations but was only correlated with salinity in LEV-B1 (negative correlation) and ALB-M'DIQ (positive correlation). Finally, Chl *a* was only significant for temporal variability at the LEV-BEY and BAL-CS stations. Although oceanic CH_4 often exhibits a strong depth dependence (Weber et al., 2019), station depth was included in our initial correlation matrix but yielded no significant relationship ($p > 0.05$). This lack of correlation indicates that CH_4 variability found among stations in our study in our study area is primarily driven by other sedimentary sources rather than depth-dependent benthic remineralization.

Our study is consistent with previous studies in the Eastern (Bange et al., 1996) and Western Mediterranean Sea (de la Paz et al., 2015, Flecha et al., 2023, 2025), where temperature was revealed to be the main controlling factor of surface N_2O and CH_4 variability.

3.4 Air-sea fluxes of N_2O and CH_4

Surface waters were consistently supersaturated with CH_4 relative to the atmosphere at all the coastal Mediterranean stations (Table 2). Consequently, the region acted as a net CH_4 source, with air-sea flux exhibiting high temporal variability (Table 3). Fluxes ranged from 0.97 to 11.41 μmol m^{-2} d^{-1} in the Balearic sub-basin, 1.74 to 15.4 μmol m^{-2} d^{-1} in the Alboran sub-basin, and reached a maximum of 35.2 μmol m^{-2} d^{-1} in the Levantine Sea (Fig. 6, Table 2). While no uniform seasonal trend was observed basin-wide, a notable regional decoupling occurred: maximum CH_4 outgassing in the Balearic sub-basin (July–November 2023) coincided with the lowest flux periods in the Alboran and Levantine sub-basins.

In contrast, N_2OSat and subsequent air-sea exchange followed a more distinct seasonal trend. Most stations remained moderately supersaturated, acting as a minor N_2O source, with the exception of brief undersaturation events (>98%) in the Balearic sub-basin in May and November 2023. N_2O fluxes peaked in the Balearic sub-basin at 2.37 μmol m^{-2} d^{-1} (January 2024), driven by a combination of supersaturation and intensified winter wind speeds in the Western Mediterranean. Overall, the N_2O flux variability mirrored seasonal concentration changes but was strongly modulated by wind-driven gas transfer.

The annual flux average (Table 3) confirmed that all stations behaved as net annual sources of both CH_4 and N_2O. The highest mean CH_4 fluxes were recorded at the Erdemli site (LEV-ETS: 13.68±9.57 μmol m^{-2} d^{-1}). At this site, the substantial discrepancy between the mean and median (8.39 μmol m^{-2} d^{-1}) highlights a heavily right-skewed distribution caused by episodically high-concentration events unique to the Levantine Sea. Conversely, annual N_2O fluxes were remarkably homogeneous across subbasins, ranging from 0.42±0.26 μmol m^{-2} d^{-1} (ALB-M'DIQ) to 1.11±0.64 μmol m^{-2} d^{-1} (BAL-PB), showing a symmetric distribution with closely aligned mean and median values.

The magnitude of the air-sea fluxes calculated in this study is consistent with the sparse literature on the Mediterranean Sea. Our CH_4 fluxes in the Alboran sub-basin (1.74 to 15.4 μmol m^{-2} d^{-1}) aligned with the ranges reported by de la Paz et al. (2015) in the Strait of Gibraltar and the recent observations by Flecha et al. (2023, 2025), who highlighted the coastal Alboran and Balearic seas as persistent sources of CH_4 emissions. The annual mean fluxes of N_2O (0.42 to 1.11 μmol m^{-2} d^{-1}) are in excellent agreement with the values reported by Bange et al. (1996) for the Aegean Sea (0.1 to 1.2 μmol m^{-2} d^{-1}), confirming that both the Eastern and Western basins act as moderate but steady sources of N_2O to the atmosphere. However, the episodic high-flux events recorded at the LEV-ETS station represent some of the highest CH_4 emission rates documented for the offshore Levantine sub-basin, emphasising the role of localised coastal hotspots in the regional greenhouse gas budget.

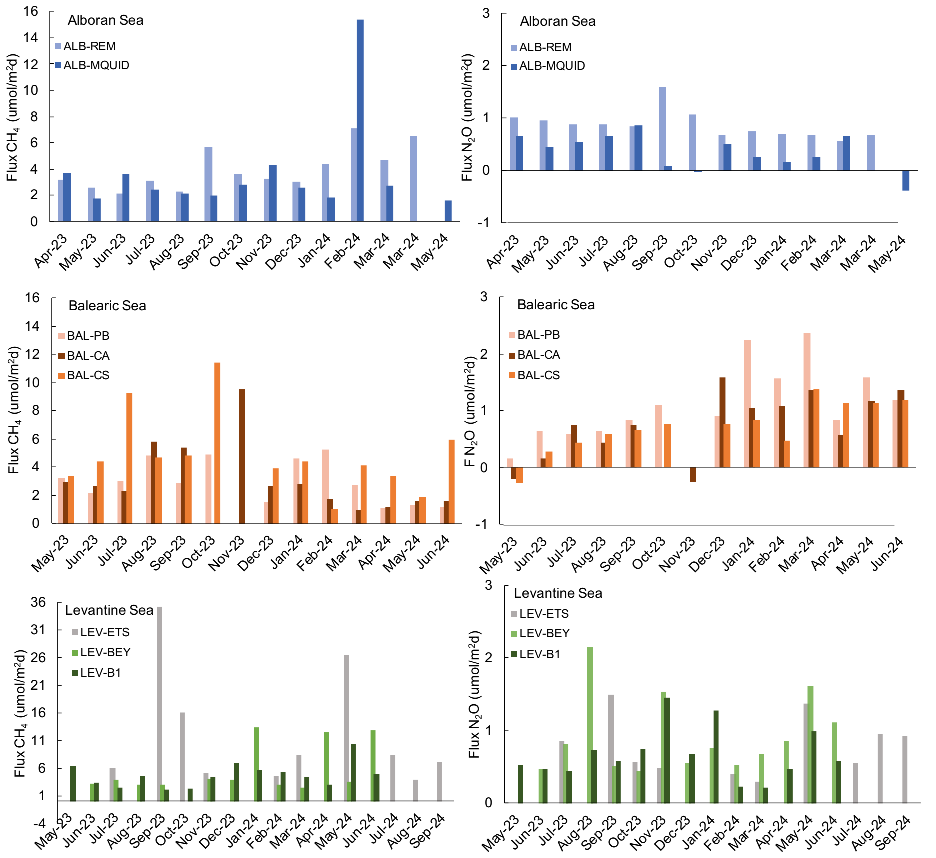

Figure 6. Time-series of air-sea fluxes of N_2O and CH_4 in nmol m^{-2} d^{-1} for each station, shown by marine ecoregions.

Table 3. Range (min-max) of air-sea fluxes for each station, and median and average annual N_2O and CH_4 air-sea flux (µmolm^{-2} d^{-1}) calculated using the expression for gas exchange rate proposed by Wanninkhof (2014).

	Site Station Code	F CH_4 (µmol m^{-2} d^{-1})			F N_2O (µmol m^{-2} d^{-1})		
		Range	**Median**	**Mean ± SD**	**Range**	**Median**	**Mean ± SD**
Balearic Sea	BAL-CA	1-9.6	2.73	3.80±2.59	-0.25-1.58	0.75	0.67±0.55
	BAL-CS	1-11.4	4.40	5.46±3.09	-0.27-1.37	0.71	0.68±0.42
	BAL-PB	1.1-5.2	3.10	3.36±1.23	0.16-2.37	0.87	1.11±0.64
Levantine Sea	LEV-B1	2.1-10.3	4.47	4.57±2.23	0.21-1.45	0.63	0.69±0.69
	LEV-BEY	2.5-13.4	3.60	4.99±3.59	0.47-2.15	0.78	0.95±0.51
	LEV-ETS	4.5-35.2	8.39	13.68±9.57	0.3-1.49	0.65	0.79±0.39
Alboran Sea	ALB-M'DIQ	1.7-15.4	2.67	3.79±3.59	-0.03-0.86	0.48	0.42±0.26
	ALB-REM	2.1-7.1	3.26	3.77±1.41	0.56-1.58	0.86	0.88±0.26

Table 4. Annual aaverage N_2O and CH_4 air-sea flux (µmolm^{-2} d^{-1}) for this study and other data published data in the Mediterranean Sea. * For the Strait of Gibraltar, the range of observed CH_4 values is presented instead of a mean due to incomplete seasonal coverage in the original study.

Region	*Reference*	*Flux CH_4 (µmol m^{-2} d^{-1})*	*Flux N_2O (µmol m^{-2} d^{-1})*
Strait of Gibraltar	de la Paz et al. (2015)	0 - 1.68 *	0.35±0.27
Balearic Sea	Flecha et al. (2023/25)	~0.2 - 9.7 (1.4±1.4)	-0.3-0.6 (0.1±0.2)
Aegean Sea	Bange et al. (1996)	0.26-14.5 (mean 1.7)	0.1 - 1.7
Alboran Sea	This study	3.8 ±3.6	0.9 ±3
Balearic Sea	This study	4.2 ±1.3	0.8±0.5
Levantine Sea	This study	7.7±5.1	0.8±0.5

4. Data availability

Data described in this paper are accessible at the Zenodo repository https://doi.org/10.5281/zenodo.19351642 (de la Paz et al.,2026).

Deleted: https://doi.org/10.5281/zenodo.19351642 (de la Paz et al.,2026). During the peer-review process, anonymous access is restricted via DOI until publication; however, data are available upon email request to the corresponding author for other interested parties

6. Conclusions

Deleted: ¶

This data paper presents the first comprehensive, seasonally-resolved dataset of N_2O and CH_4 concentrations and air-sea fluxes across under-sampled coastal regions of the Mediterranean Sea. Our results confirm that these coastal waters consistently act as a net source of both N_2O and CH_4 to the atmosphere. We found a strong thermodynamic control on N_2O variability, with higher concentrations in colder waters and moderate oversaturation throughout the Mediterranean Sea. In contrast, CH_4 dynamics were highly variable, positively correlated with temperature, and marked by episodic high-flux events, particularly in the Levantine Sea, indicating the influence of localized geological or anthropogenic sources. Despite challenges in assessing changes in N_2O and CH_4 in coastal water due to limited measurements, this dataset contributes to the understanding of greenhouse gas variability in the region. This quality-controlled ROADSTER dataset provides a valuable regional resource that enables accurate trend quantification and change estimation, serving as an essential baseline for evaluating environmental impacts, refining regional non-CO_2 greenhouse gas budgets, and improving global climate models.

11. Author contribution

MdlP conducted the sample analyses, performed the data analyses, and wrote the first draft of the manuscript. SF, FB, MF, VI, KÖ, and IEH collected samples. SF, MdP and AERH contributed to the design of the study. FFP contributed to data analysis. IEH designed and led the study. All authors contributed to discussions on sample design and collection and data analysis, and reviewed, revised, and approved the final version of the manuscript.

12. Competing interests

The contact author has declared that none of the authors has any competing interests

15. Acknowledgements

Data has been collected and analysed within the project *COOPB22023 of the i-COOP 2022* call from the Spanish Research Council (CSIC). Sampling in the Balearic Sea has been enabled through the Balearic Ocean Acidification Time Series (BOATS) with financial support of PID2021-123723OB-C22 (CYCLE) funded by MCIN/AEI/10.13039/501100011033 "ERDF A way of making Europe". The present research has been carried out in the framework of the activities of the Spanish Government through the accreditation "Centro de Excelencia María de Maeztu" to IMEDEA (CSIC-UIB)

(CEX2021-001198). VI and KO received logistic and historical data support from DEKOSIM (BAP-08-11-DPT2012K120880) and TÜBİTAK project no 120Y082 and would like to express gratitude to Kazım Tutsak, Alaeddin Akkaş, Serhat Ertuğrul, Ganiye Ekmekçi for the sampling efforts at Erdemli stations and to Mr. Ismail Ennaskhi from the Tangier Regional Center and Mr. Ahmed Chihani from the Nador Regional Center for their help during the samplings in Morocco. Thanks to X.A. Padin for his assistance providing the data-product wind data CCMP. MdlP acknowledges the financial support for the contracts financed by the Spanish Ministry of Science under grant PTA2024-025174-I. SF staff hired under the Generation D initiative, promoted by Red.es, an organization affiliated with the Ministry for Digital Transformation and the Civil Service, financed by the Recovery, Transformation, and Resilience Plan through the European Union's Next Generation funds. This work contributes to the CSIC Interdisciplinary Thematic Platform, OCEANS+.

Deleted:

16. References

Bange, H. W., Rapsomanikis, S., and Andreae, M. O.: The Aegean Sea as a source of atmospheric nitrous oxide and methane, Marine Chemistry, 53, 41–49, https://doi.org/10.1016/0304-4203(96)00011-4, 1996.

Bange, H. W., Arévalo-Martínez, D. L., de la Paz, M., Farías, L., Kaiser, J., Kock, A., Law, C. S., Rees, A. P., Rehder, G., Tortell, P. D., Upstill-Goddard, R. C., and Wilson, S. T.: A Harmonized Nitrous Oxide (N2O) Ocean Observation Network for the 21st Century, Front. Mar. Sci., 6, https://doi.org/10.3389/fmars.2019.00157, 2019.

Bendshneider K. and Robinson, R.-J. A new spectrophotometric method for the determination of nitrite in sea water. J. Mar. Res., 11, pp. 87-96, 1952

Bianchi, C. N. and Morri, C.: Marine Biodiversity of the Mediterranean Sea: Situation, Problems and Prospects for Future Research, Marine Pollution Bulletin, 40, 367–376, https://doi.org/10.1016/S0025-326X(00)00027-8, 2000.

Champenois, W. and Borges, A. V.: Net community metabolism of a Posidonia oceanica meadow, Limnology and Oceanography, 66, 2126–2140, https://doi.org/10.1002/lno.11724, 2021.

Charpentier, J., Farias, L., Yoshida, N., Boontanon, N., and Raimbault, P.: Nitrous oxide distribution and its origin in the central and eastern South Pacific Subtropical Gyre, Biogeosciences, 4, 729–741, https://doi.org/10.5194/bg-4-729-2007, 2007.

Ciais, P., Sabine, C., Bala, G., Bopp, L., Brovkin, V., Canadell, J., Chhabra, A., DeFries, R., Galloway, J., Heimann, M., Jones, C., Le Quéré, C., Myneni, R. B., Piao, S., and Thornton, P.: Carbon and other biogeochemical cycles, in: Climate Change 2013: The Physical Science Basis. Contribution of Working Group I to the Fifth Assessment Report of the Intergovernmental Panel on Climate Change. [Stocker, T.F., D. Qin, G.-K. Plattner, M. Tignor, S.K. Allen, J. Boschung, A. Nauels, Y. Xia, V. Bex and P.M. Midgley (eds.)]. Cambridge University Press, Cambridge, United Kingdom and New York, NY, USA, 465–570, 2013.

Codispoti, L. A.: Interesting Times for Marine N2O, Science, 327, 1339–1340, https://doi.org/10.1126/science.1184945, 2010.

Coleman, D. F. and Ballard, R. D.: A highly concentrated region of cold hydrocarbon seeps in the southeastern Mediterranean Sea, Geo-Mar Lett, 21, 162–167, https://doi.org/10.1007/s003670100079, 2001.

de la Paz, M., Huertas, I. E., Flecha, S., Ríos, A. F., and Pérez, F. F.: Nitrous oxide and methane in Atlantic and Mediterranean waters in the Strait of Gibraltar: Air-sea fluxes and inter-basin exchange, Progress in Oceanography, 138, Part A, 18–31, https://doi.org/10.1016/j.pocean.2015.09.009, 2015.

de la Paz, M., Flecha, S., Bouthir, Fatima. Zohra, Fakhri, M., Hassoun, A. E. R., Ibello, V., Özkan, K., Fernandez Perez, F., Adil, C., & Hendriks, I. (2026). Nitrous oxide and methane concentrations and air-sea fluxes in undersampled areas of the Mediterranean basin [Data set]. Zenodo. https://doi.org/10.5281/zenodo.19351642

de la Paz, M., Pérez, F. F., and Oceanografía (IIM-CSIC), D. de: Servicio de análisis de gases de efecto invernadero en aguas naturales (AQUANITROMET), Greenhouse gas analysis service in natural waters (AQUANITROMET), 2026.

Damm, E., Thoms, S., Beszczynska-Möller, A., Nöthig, E. M., and Kattner, G.: Methane excess production in oxygen-rich polar water and a model of cellular conditions for this paradox, Polar Science, 9, 327–334, https://doi.org/10.1016/j.polar.2015.05.001, 2015.

Dickson, A. and Goyet, C.: Handbook of methods for the analysis of the various parameters of the carbon dioxide system in sea water. Version 2, https://doi.org/10.2172/10107773, 1994.

Doney, S. C.: The growing human footprint on coastal and open-ocean biogeochemistry, Science, 328, 1512–1516, 2010.

EEA. (2020). *Multiple pressures and their combined effects in Europe's seas*. European Environment Agency.

Escudier, R., Clementi, E., Omar, M., Cipollone, A., Pistoia, J., Aydogdu, A., Drudi, M., Grandi, A., Lyubartsev, V., Lecci, R., Cretí, S., Masina, S., Coppini, G., & Pinardi, N.: Mediterranean Sea Physical Reanalysis (CMEMS MED-Currents) (Version 1) [Data set]. Copernicus Monitoring Environment Marine Service (CMEMS). https://doi.org/10.25423/CMCC/MEDSEA_MULTIYEAR_PHY_006_004_E3R1, 2020).

Fach, B. A., Orek, H., Yilmaz, E., Tezcan, D., Salihoglu, I., Salihoglu, B., and Latif, M. A.: Water Mass Variability and Levantine Intermediate Water Formation in the Eastern Mediterranean Between 2015 and 2017, Journal of Geophysical Research: Oceans, 126, e2020JC016472, https://doi.org/10.1029/2020JC016472, 2021.

Flecha, S., Rueda, D., de la Paz, M., Pérez, F. F., Alou-Font, E., Tintoré, J., and Hendriks, I. E.: Spatial and temporal variation of methane emissions in the coastal Balearic Sea, Western Mediterranean, Science of The Total Environment, 865, 161249, https://doi.org/10.1016/j.scitotenv.2022.161249, 2023.

Flecha, S., de la Paz, M., Pérez, F. F., Marbà, N., Morell, C., Alou-Font, E., Tintoré, J., and Hendriks, I. E.: Drivers of the spatiotemporal distribution of dissolved nitrous oxide and air–sea exchange in a coastal Mediterranean area, Ocean Science, 21, 1515–1532, https://doi.org/10.5194/os-21-1515-2025, 2025.

Freing, A., Wallace, D. W. R., and Bange, H. W.: Global oceanic production of nitrous oxide, Phil. Trans. R. Soc. B, 367, 1245–1255, https://doi.org/10.1098/rstb.2011.0360, 2012.

Grasshoff, K., Ehrhardt, M., and Kremling, K.: Methods of Seawater Analysis, 2nd ed., Verlag Chemie, Weinheim, Germany, 1983.

Hansen, H. P.: Determination of oxygen, in: Methods of Seawater Analysis, John Wiley & Sons, Ltd, 75–89, https://doi.org/10.1002/9783527613984.ch4, 1999.

Hassoun, A. E. R., Gemayel, E., Krasakopoulou, E., Goyet, C., Abboud-Abi Saab, M., Guglielmi, V., Touratier, F., and Falco, C.: Acidification of the Mediterranean Sea from anthropogenic carbon penetration, Deep Sea Research Part I: Oceanographic Research Papers, 102, 1–15, https://doi.org/10.1016/j.dsr.2015.04.005, 2015.

Field Code Changed

Hassoun, A. E. R., Hernández-Moresino, R., Barbieri, E. S., Carbajal, J. C., and Crespi-Abril, A.: Coastal Monitoring in the Context of Climate Change: Time-Series Efforts in Lebanon and Argentina, Oceanography, 34, 12–13, https://doi.org/10.5670/oceanog.2021.supplement.02-05, 2022.

Hassoun, A. E. R., Tanhua, T., Heslop, E., Lips, I., Álvarez, M., Petihakis, G., García-Ibáñez, M. I., Velaoras, D., Giani, M., Bange, H. W., Lønborg, C., and Karstensen, J.: A first scoring approach for evaluating the European Ocean Observing Community, Front. Mar. Sci., 11, https://doi.org/10.3389/fmars.2024.1466820, 2024.

Kuyumcu, B. (2023). Estimating submarine groundwater discharge in the Cilician Basin by radioactive isotope tracers and hydrodynamic modeling (Master's thesis, Middle East Technical University). (METU Open Access handle: 11511/104884).

Lorenzen, C. J.: Determination of Chlorophyll and Pheo-Pigments: Spectrophotometric Equations, Limnology and Oceanography, 12, 343–346, https://doi.org/10.4319/lo.1967.12.2.0343, 1967.

Mears, C.; Lee, T.; Ricciardulli, L.; Wang, X.; Wentz, F., 2022: RSS Cross-Calibrated Multi-Platform (CCMP) 6-hourly ocean vector wind analysis on 0.25 deg grid, Version 3.0, Remote Sensing Systems, Santa Rosa, CA. Available at www.remss.com https://doi.org/10.56236/RSS-uv6h30

Merey, Ş. and Longinos, S. N.: The gas hydrate potential of the Eastern Mediterranean basin, Bull.Min.Res.Exp., 160, 117–134, https://doi.org/10.19111/bulletinofmre.502275, 2019.

MedECC (2020). Climate and Environmental Change in the Mediterranean Basin – Current Situation and Risks for the Future. First Mediterranean Assessment Report [Cramer, W., Guiot, J., Marini, K. (eds.)] Union for the Mediterranean, Plan Bleu, UNEP/MAP, Marseille, France, 632pp, ISBN 978-2-9577416-0-1, doi: 10.5281/zenodo.4768833

Mouillot, D., Albouy, C., Guilhaumon, F., Ben Rais Lasram, F., Coll, M., Devictor, V., Meynard, C. N., Pauly, D., Tomasini, J. A., Troussellier, M., Velez, L., Watson, R., Douzery, E. J. P., and Mouquet, N.: Protected and Threatened Components of Fish Biodiversity in the Mediterranean Sea, Current Biology, 21, 1044–1050, https://doi.org/10.1016/j.cub.2011.05.005, 2011.

Murphy, J. and Riley, J. P.: A modified single solution method for the determination of phosphate in natural waters, Analytica Chimica Acta, 27, 31–36, https://doi.org/10.1016/S0003-2670(00)88444-5, 1962.

Ouba, A., Saab, M. A.-A., and Stemmann, L.: Temporal Variability of Zooplankton (2000-2013) in the Levantine Sea: Significant Changes Associated to the 2005-2010 EMT-like Event?, PLOS ONE, 11, e0158484, https://doi.org/10.1371/journal.pone.0158484, 2016.

Pisano, A., Marullo, S., Artale, V., Falcini, F., Yang, C., Leonelli, F. E., Santoleri, R., and Buongiorno Nardelli, B.: New Evidence of Mediterranean Climate Change and Variability from Sea Surface Temperature Observations, Remote Sensing, 12, 132, https://doi.org/10.3390/rs12010132, 2020.

Reeburgh, W. S.: Oceanic Methane Biogeochemistry, Chem. Rev., 107, 486–513, https://doi.org/10.1021/cr050362v, 2007.

Rees, A. P., Bange, H. W., Arévalo-Martínez, D. L., Artioli, Y., Ashby, D. M., Brown, I., Campen, H. I., Clark, D. R., Kitidis, V., Lessin, G., Tarran, G. A., and Turley, C.: Nitrous oxide and methane in a changing Arctic Ocean, Ambio, 51, 398–410, https://doi.org/10.1007/s13280-021-01633-8, 2022.

Resplandy, L., Hogikyan, A., Müller, J. D., Najjar, R. G., Bange, H. W., Bianchi, D., Weber, T., Cai, W.-J., Doney, S. C., Fennel, K., Gehlen, M., Hauck, J., Lacroix, F., Landschützer, P., Le Quéré, C., Roobaert, A., Schwinger, J., Berthet, S., Bopp, L., Chau, T. T. T., Dai, M., Gruber, N., Ilyina, T., Kock, A., Manizza, M., Lachkar, Z., Laruelle, G. G., Liao, E., Lima, I. D., Nissen, C., Rödenbeck, C., Séférian, R., Toyama, K., Tsujino, H., and Regnier, P.: A Synthesis of Global Coastal Ocean Greenhouse Gas Fluxes, Global Biogeochemical Cycles, 38, e2023GB007803, https://doi.org/10.1029/2023GB007803, 2024.

Rosentreter, J. A., Borges, A. V., Deemer, B. R., Holgerson, M. A., Liu, S., Song, C., Melack, J., Raymond, P. A., Duarte, C. M., Allen, G. H., Olefeldt, D., Poulter, B., Battin, T. I., and Eyre, B. D.:

Field Code Changed

Half of global methane emissions come from highly variable aquatic ecosystem sources, Nat. Geosci., 14, 225–230, https://doi.org/10.1038/s41561-021-00715-2, 2021.

Rosentreter, J. A., Laruelle, G. G., Bange, H. W., Bianchi, T. S., Busecke, J. J. M., Cai, W.-J., Eyre, B. D., Forbrich, I., Kwon, E. Y., Maavara, T., Moosdorf, N., Najjar, R. G., Sarma, V. V. S. S., Van Dam, B., and Regnier, P.: Coastal vegetation and estuaries are collectively a greenhouse gas sink, Nat. Clim. Chang., 13, 579–587, https://doi.org/10.1038/s41558-023-01682-9, 2023.

Saunois, M., Stavert, A. R., Poulter, B., Bousquet, P., Canadell, J. G., Jackson, R. B., Raymond, P. A., Dlugokencky, E. J., Houweling, S., Patra, P. K., Ciais, P., Arora, V. K., Bastviken, D., Bergamaschi, P., Blake, D. R., Brailsford, G., Bruhwiler, L., Carlson, K. M., Carrol, M., Castaldi, S., Chandra, N., Crevoisier, C., Crill, P. M., Covey, K., Curry, C. L., Etiope, G., Frankenberg, C., Gedney, N., Hegglin, M. I., Höglund-Isaksson, L., Hugelius, G., Ishizawa, M., Ito, A., Janssens-Maenhout, G., Jensen, K. M., Joos, F., Kleinen, T., Krummel, P. B., Langenfelds, R. L., Laruelle, G. G., Liu, L., Machida, T., Maksyutov, S., McDonald, K. C., McNorton, J., Miller, P. A., Melton, J. R., Morino, I., Müller, J., Murguia-Flores, F., Naik, V., Niwa, Y., Noce, S., O'Doherty, S., Parker, R. J., Peng, C., Peng, S., Peters, G. P., Prigent, C., Prinn, R., Ramonet, M., Regnier, P., Riley, W. J., Rosentreter, J. A., Segers, A., Simpson, I. J., Shi, H., Smith, S. J., Steele, L. P., Thornton, B. F., Tian, H., Tohjima, Y., Tubiello, F. N., Tsuruta, A., Viovy, N., Voulgarakis, A., Weber, T. S., van Weele, M., van der Werf, G. R., Weiss, R. F., Worthy, D., Wunch, D., Yin, Y., Yoshida, Y., Zhang, W., Zhang, Z., Zhao, Y., Zheng, B., Zhu, Q., Zhu, Q., and Zhuang, Q.: The Global Methane Budget 2000–2017, Earth System Science Data, 12, 1561–1623, https://doi.org/10.5194/essd-12-1561-2020, 2020.

Sommer, M., Bange, H. W., Eisnecker, P., Schulz, G., Stoltenberg, I., and Arévalo-Martínez, D. L.: N2O Emissions From the Eastern Tropical Indian Ocean, Geophysical Research Letters, 52, e2025GL117627, https://doi.org/10.1029/2025GL117627, 2025.

Strickland J.D.H. and Parsons, T.R., A practical handbook of seawater analysis. Bull. Fish. Res. Board Can., 167 (1968), p. 311, 1968.

Tanhua, T., Pouliquen, S., Hausman, J., O'Brien, K., Bricher, P., de Bruin, T., Buck, J. J. H., Burger, E. F., Carval, T., Casey, K. S., Diggs, S., Giorgetti, A., Glaves, H., Harscoat, V., Kinkade, D., Muelbert, J. H., Novellino, A., Pfeil, B., Pulsifer, P. L., Van de Putte, A., Robinson, E., Schaap, D., Smirnov, A., Smith, N., Snowden, D., Spears, T., Stall, S., Tacoma, M., Thijsse, P., Tronstad, S., Vandenberghe, T., Wengren, M., Wyborn, L., and Zhao, Z.: Ocean FAIR Data Services, Front. Mar. Sci., 6, https://doi.org/10.3389/fmars.2019.00440, 2019.

Tintoré, J., Gomis, D., Alonso, S., and Parrilla, G.: Mesoscale Dynamics and Vertical Motion in the Alborán Sea, Journal of Physical Oceanography, 21, 811–823, https://doi.org/10.1175/1520-0485(1991)021<0811:MDAVMI>2.0.CO;2, 1991.

Viúdez, A., Pinot, J.-M., and Haney, R. L.: On the upper layer circulation in the Alboran Sea, Journal of Geophysical Research: Oceans, 103, 21653–21666, https://doi.org/10.1029/98JC01082, 1998.

Wanninkhof, R.: Relationship between wind speed and gas exchange over the ocean revisited: Gas exchange and wind speed over the ocean, Limnol. Oceanogr. Methods, 12, 351–362, https://doi.org/10.4319/lom.2014.12.351, 2014.

Weber, T., Wiseman, N. A., and Kock, A.: Global ocean methane emissions dominated by shallow coastal waters, Nat Commun, 10, 4584, https://doi.org/10.1038/s41467-019-12541-7, 2019.

Wilson, S. T., Bange, H. W., Arévalo-Martínez, D. L., Barnes, J., Borges, A. V., Brown, I., Bullister, J. L., Burgos, M., Capelle, D. W., Casso, M., de la Paz, M., Farías, L., Fenwick, L., Ferrón, S., Garcia, G., Glockzin, M., Karl, D. M., Kock, A., Laperriere, S., Law, C. S., Manning, C. C., Marriner, A., Myllykangas, J.-P., Pohlman, J. W., Rees, A. P., Santoro, A. E., Tortell, P. D., Upstill-Goddard, R. C., Wisegarver, D. P., Zhang, G.-L., and Rehder, G.: An intercomparison of oceanic methane and nitrous oxide measurements, Biogeosciences, 15, 5891–5907, https://doi.org/10.5194/bg-15-5891-2018, 2018.